PRJ4/LCT4-4L
Late-News Paper
Invited

Transmissive compact spatial polarization converter to generate polarization distribution with arbitrary phase and polarization on a Poincaré sphere

Keisuke Yoshiki[1], Takeshi Yamamoto[2]

yoshiki@eng.u-hyogo.ac.jp
[1]Institute for Research Promotion and Collaboration, University of Hyogo
9301 Incubation Center, 2167 Shosha, Himeji, Hyogo 6712201
[2]Oasa Electronics Co.,Ltd
3817-10,Kitahiroshima-cho,Yamagata-gun,Hiroshima,Japan
Keywords: full Poincaré polarization control, spatial light modulator, optical measurement, laser machining

ABSTRACT

We have developed a transmissive optical modulator with arbitrary control of polarization and phase. The phase control range exceeds 6π, and the polarization is fully controllable on Poincaré sphere. The installation is completed by simply inserting the device into the optical path of an existing optical device. This paper describes its principle, performance, and potential application to high power lasers.

1 Introduction

Applications of cylindrical vector beams, that have polarization and phase distribution in the beam, such as radially polarized light, azimuthally polarized light, and optical vortices, have been proposed for various applications, including microscopy[1-3] laser processing[4], optical communications[5], optical trapping[6], and particle acceleration[7].

However, because of the complexed and large equipment required, we have implemented a compact liquid crystal device in microscopes to generate radial and azimuthal polarization, adding new abilities to an extant instrument (8-12). In addition, a higher degree of freedom of polarization has been required in recent years. In particular, full Poincaré beams, in which all polarizations are included in the beam, have been proposed and are attracting attention. To meet this requirement, we have proposed a transmission-type liquid crystal polarization device that can generate polarizations corresponding to all points on the Poincaré sphere.

We have also developed a liquid crystal device that improves the detection capability of an imaging camera device by installing the liquid crystal, and a liquid crystal that can be attached to a high-power laser used in a laser processing system.This device is already commercially available as polarization mode converter (PMC) , and is significantly implementable to preexisting optical equipment and more cost-effective than its Liquid crystal on silicon (LCOS) based counterparts.

2 Principle

The arrangement of PMC is shown in Fig. 1. This device is composed of three transmissive ECB（Electrically Controlled Birefringence）liquid crystal cells which control phase difference between a and b axis. The axis a is controllable, and the axis b is uncontrollable axis. These liquid crystal cells are called LC1, LC2, and LC3 in order from the side closer to the light source. LC1, LC2, and LC3 were arranged that the controllable axes of each liquid crystal were parallel, 45°, and parallel to the incident linearly polarized light in order from the incident side, respectively. The phase is controlled by LC1, and the polarization is controlled by combining LC2 and LC3. Each liquid crystal cells have concentric and radial divided segments

Each liquid crystal cell has concentrically and radially separated segments of the same shape, which are stacked so that the corresponding segments are overlapped. Since each liquid crystal is a static liquid crystal, each segment can be driven independently. Therefore, arbitrary polarization and phase can be specified for the region corresponding to each segment. As a result, various polarization and phase distributions are generated.

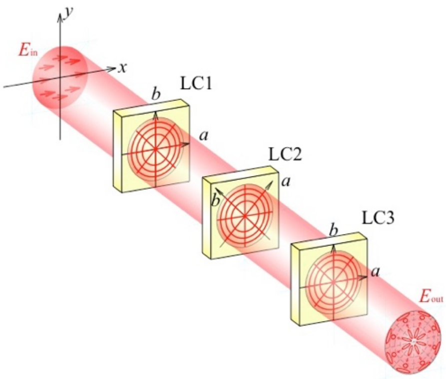

Fig. 1 Optical arrangement for generating arbitrary phase and polarization distributions

the Jones matrix of a liquid crystal cells are represented as

$$L(x)=\begin{bmatrix} e^{-ix} & 0 \\ 0 & 1 \end{bmatrix} \tag{1}$$

when the controllable axis is oriented horizontally. The birefringence phase difference x is given as a function $x(V, f)$ corresponding to the voltage amplitude V and the frequency f, and is determined by calibration tests after fabrication. An example of the result is shown in Figure 2. Fig. 2 shows the variation of x for each amplitude and frequency of the drive voltage when driven by a sinusoidal voltage, and it can be seen that more than two control quantities can be obtained in both amplitude and frequency control.

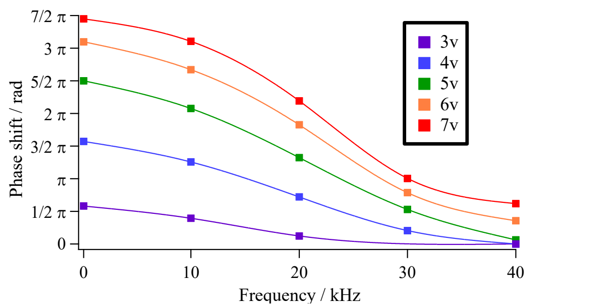

Fig. 2 Phase difference control of ECB liquid crystal by driving voltage and frequency

Figure 1 is a case where the liquid crystal is divided into 32 concentric and radial segments. The n-divided pixels are numbered i=0,..., n-1, and the light rays pass through the pixels with the same number i, since the pixels with the same number overlap each other between the liquid crystal elements. In this configuration, the ejection polarization from the PMC is given by the following equation.

$$\begin{aligned} E_{out} &= L(\zeta_i)\,R\left(-\frac{\pi}{4}\right)L(\eta_i)\,R\left(\frac{\pi}{4}\right)L(\xi_i)\begin{bmatrix}1\\0\end{bmatrix} \\ &= \begin{bmatrix} e^{-i\zeta_i} & 0 \\ 0 & 1 \end{bmatrix}\frac{1}{2}e^{-i\xi_i}\begin{bmatrix} 1+e^{-i\eta_i} \\ 1-e^{-i\eta_i} \end{bmatrix} \\ &= \frac{1}{2}e^{-i\xi_i}\begin{bmatrix} e^{-i\zeta_i}\left(1+e^{-i\eta_i}\right) \\ \left(1-e^{-i\eta_i}\right) \end{bmatrix} \end{aligned} \tag{2}$$

where R(θ)is the rotation matrix, and is the counterclockwise rotation angle as seen by the observer, denoted by

$$R(\theta)=\begin{bmatrix} \cos\theta & \sin\theta \\ -\sin\theta & \cos\theta \end{bmatrix} \tag{3}$$

The extinction ratio (the reciprocal of the ellipticity A) is A-1, the azimuthal angle of the elliptical polarization, and the phase in the direction of the elliptical major axis are denoted by

$$\Phi=\frac{1}{2}\tan^{-1}\left(-\tan\eta\sin\zeta\right) \tag{4}$$

$$A=\tan\left\{\frac{1}{2}\sin^{-1}\left(\sin\eta\cos\zeta\right)\right\} \tag{5}$$

$$\Theta=-\xi-\eta-\zeta+\tan^{-1}\left\{\cos\eta\tan\left(\zeta-\frac{\pi}{2}\right)\right\} \tag{6}$$

where the pixel numbers are omitted. If the polarization is controlled by LC2 and LC3, the phase is also affected. To compensate for this, the phase is shifted beforehand by LC1, and then the necessary phase is added to form an arbitrary phase distribution.

We now show that the polarization states represented by this equation cover all the polarization states that can be represented by the Jones vector.

Eliminating equations 4 and 6 leads to the relation

$$\tan^2 2\Phi=\frac{\sin^2\eta-\sin^2\left(2\tan^{-1}A\right)}{\cos^2\eta}. \tag{7}$$

Since the possible range of A is 0≦A<1, by controlling η with a width of 0≦η<2π, it is possible to rotate Φ with a control width of 0≦Φ<π while maintaining the desired extinction ratio R. At the same time, the required control width becomes 0≦ζ<π.

These results are summarized in Fig. 3. This figure shows the shape of the polarization when the horizontal and vertical axes are changed in steps of π/8, respectively, with solid lines for clockwise polarization and dashed lines for counterclockwise polarization, and at the same time the extinction ratio is shown in color scale. The extinction ratio is also shown in color scale.

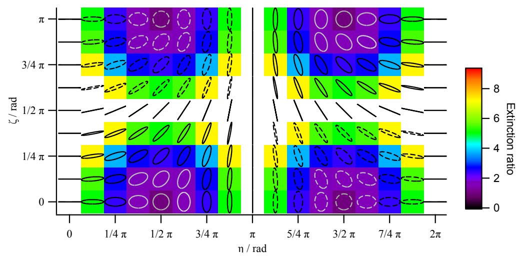

Fig. 3 Dependence of the phase difference between LC2, LC3 and the polarization generated by the PMC

From this figure, we can visually see that polarization of all ellipticities, from linear to circular, can be generated for all azimuthal angles. The old PMC corresponds to the one in which LC3 is fixed at ζ=π/2 and replaced by λ/4 plate.

3 Results

Figure 4 shows the experimental results of the polarization produced by PMC. The center wavelength is 520 nm with a bandwidth of 10 nm. The elliptical major axis direction was controlled in 1° steps from 0 to 180°, and the extinction ratio (ratio of light intensity in the major axis direction to that in the minor axis direction) was set to 50^x. x is controlled in 1° steps between 0 and 50. The accuracy was adjusted so that the ellipse major axis direction was ±0.5° and the extinction ratio was ±0.5 relative to the x value.

Fig. 4(a) shows the elliptical major axis direction and

Fig. 4(b) shows the extinction ratio. There are missing data in the region close to the circular polarization. As shown in Fig. 3, the more the polarization is close to circular polarization, the narrower the phase control range to rotate the polarization becomes, and thus the electrical resolution of the driver circuit becomes insufficient. Therefore, if the generated polarization is too far from the requirement, it is treated as invalid data. Since the valid data covers 99% of the total, it represents almost all the polarization states generated in this range.

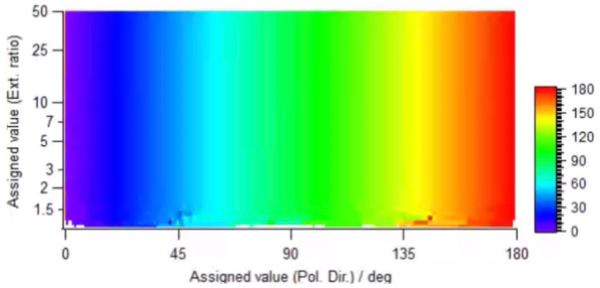

(a) elliptical major axis direction

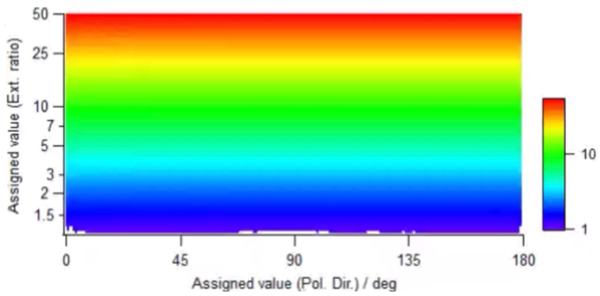

(b) extinction ratio

Fig. 4 Measured polarization relative to assigned polarization

As a demonstration of generating polarization distribution with a segmented PMC, polarization control was performed using a radially divided liquid crystal with eight segments, and the results were recorded by a polarization camera. The results are shown in Fig. 4. A movie (https://studio.youtube.com/video/IGChM4l2Ixo/) is also available. The display of the polarization camera is shown in HSL color scale, with hue indicating the angle of polarization (AOP) and lightness indicating the degree of linear polarization (DOLP). In total, there are nine steps. The correspondence between the HSL hue diagram and the polarization state is shown in Fig. 5(m).

Figs. 4(a)-(h) are images in which all segments are linearly polarized and their AOPs are rotated from 0 to 157.5° in 22.5° steps. Fig. 4(i) and (j) show the circular polarization of CW and CCW, respectively. However, these two polarizations are indistinguishable with a polarization camera, and can be distinguished by inserting a waveplate.

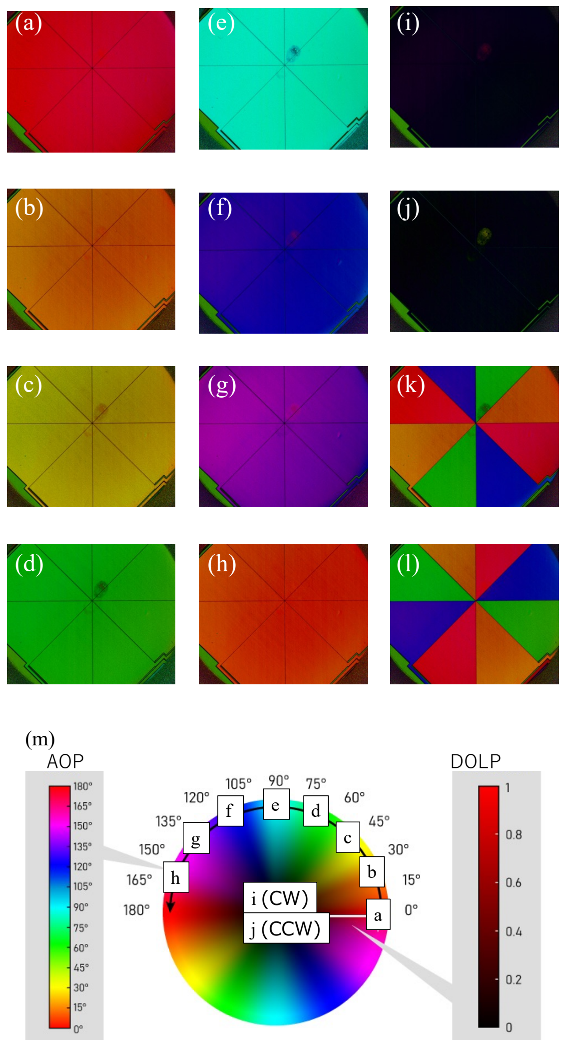

Fig. 5 Polarization distribution control by an eight-segment PMC

4 LC for kW laser application

One of the features of PMC is that it is applicable to kW lasers. Conventional liquid crystals are not able to resist laser irradiation of several tens of watts. The reason for the destruction is the heat generated by the light passing through the liquid crystal. The liquid crystals that consist of PMC absorb a small amount of light, 1.31% for the liquid crystals and 0.14% for the ITO. Assuming a 3kW laser output, 43.5 W of heat is generated. In the temperature range where liquid crystals is available, the cooling mechanism is mainly thermal conduction, and convection and radiation have negligible effects. Therefore, the liquid crystal is cooled by heat conduction through the substrate to the housing. However, since the thermal conductivity of the glass used as the liquid crystal substrate is not sufficient, heat accumulates inside the liquid crystal, leading to destruction by cracks in the substrate. However, under kW laser irradiation, the heat accumulates inside the liquid crystal because the thermal conductivity of the glass substrate is not sufficient, leading to destruction by cracking of the substrate. Therefore, sapphire substrates for liquid crystals were used instead of glass. Since sapphire has 56 times higher thermal conductivity than glass, thermal resistance to high-power lasers is improved. Figure 6 shows the results of simulation and experiment. Fig. 6(a) shows a cross-section of the water-cooled enclosure that cools the liquid crystal elements. Using this model, time series calculations of the maximum and minimum temperatures of the liquid crystal were performed under several cooling water flow rates. As a result, the increased temperature is suppressed to about 10-12°C, which shows that the liquid crystal is applicable to the 3 kW output laser. As a confirmation of the simulation, the surface temperature of the liquid crystal cell was measured by thermography under the laser irradiation Fig. 6(c) shows the results of the measurement. The temperature of the liquid crystal cell under 3 kW laser irradiation is in excellent agreement with the simulation, and the liquid crystal is kept at a temperature sufficient for operation up to 6 kW.

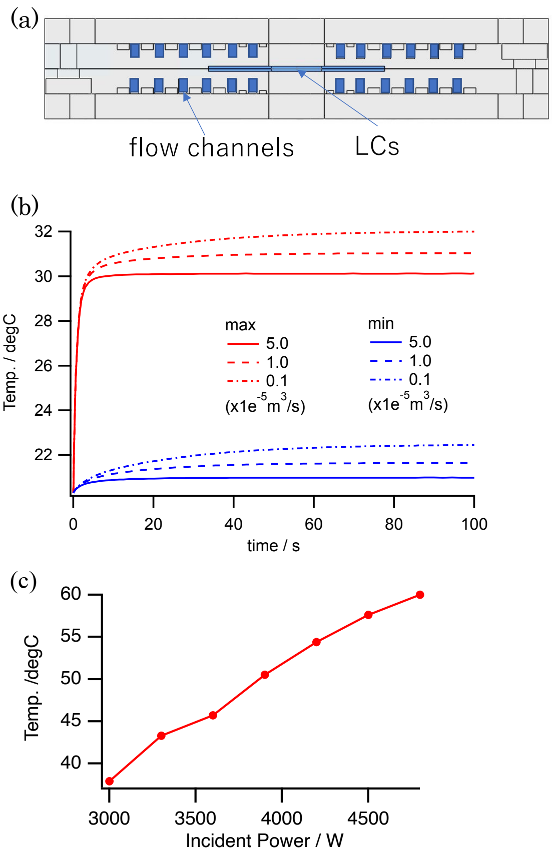

Fig. 6 Temperature at kW laser incidence

Fig. 7(a) shows the temperature distribution of the liquid crystal irradiated by a 4 mm diameter laser. 24.2°C temperature difference was generated. Fig. 7(b) is a polarization camera image of the polarization generated by the liquid crystal.

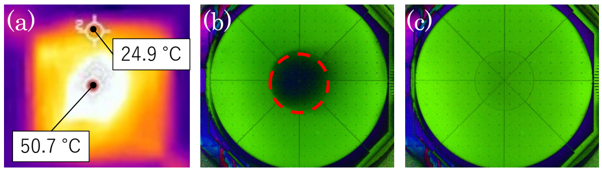

Fig. 7 Variation of liquid crystal characteristics with temperature elevations and its correction

Although the liquid crystal is configured to generate linear polarization for all segments, the area within the dashed line where the laser enters is nearly circularly polarized due to the temperature elevation. Since this liquid crystal has 16 segments (8 inner segments and 8 outer segments), the temperature effect was compensated by adjusting the voltage of the inner segments. As a result, a uniform polarization distribution was obtained as shown in Fig. 7(c). By increasing the number of segments, even a continuous temperature distribution can be corrected.

5 Conclusions

We have developed a transmission-type liquid crystal polarization/phase device that is installed in optical devices for a variety of applications. It was experimentally confirmed that polarization is controlled arbitrarily, and that it is available for high-power light. In particular, the application to high-power laser processing, which has been growing remarkably in recent years, has great potential.

References

[1] T. G. Brown, “Progress in Optics” 56, Chap.3 81 (2011).
[2] C. J. R. Sheppard, and A. Choudhury, “Annular pupils, radial polarization, and superresolution” Appl. Opt., Vol. 43, pp. 4322-4327 (2004).
[3] K. Yoshiki, M. Hashimoto and T. Araki, “Second-Harmonic-Generation Microscopy Using Excitation Beam with Controlled Polarization Pattern to Determine Three-Dimensional Molecular Orientation”, Jpn. J. Appl. Phys., Vol. 44, pp. 1066-1068 (2005).
[4] Y. Kozawa and S. Sato, “Focusing property of a double-ring-shaped radially polarized beam” Opt. Lett. Vol. 31, pp. 820-822 (2006).
[5] B. Tan and K. Venkatakrishnan., “Interconnect microvia drilling with a radially polarized laser beam”J. Micromech. Microeng., Vol. 16, pp. 2603-2607 (2006).
[6] G. Milione et al., “Using the nonseparability of vector beams to encode information for optical communication”, Opt. Lett. Vol. 40, pp. 1980-1983 (2015).
[7] S. Sato, Y. Harada, and Y.Waseda, “Optical trapping of microscopic metal particles”, Opt. Lett., Vol. 19, pp, 1807-1807 (1994).